Cross sections for electron scattering from sulfuryl chloride fluoride (SO$_2$ClF) molecules

Czesław Szmytkowski, Paweł Możejko, Stanisław Kwitnewski, Elżbieta Ptasińska-Denga and Alicja Domaracka

Atomic Physics Group, Department of Atomic Physics and Luminescence, Faculty of Applied Physics and Mathematics, Gdańsk University of Technology, ul. Gabriela Narutowicza 11/12, 80-952 Gdańsk, Poland

E-mail: czsz@mif.pg.gda.pl

Abstract
Absolute total cross section (TCS) for electron scattering from sulfuryl chloride fluoride (SO$_2$ClF) molecules was measured in a linear transmission experiment at energies ranging from 0.6 to 370 eV. The experimental TCS energy function has a deep minimum (30×10^{-20} m^2) at 3 eV which separates two distinct TCS enhancements. Below 3 eV the TCS curve increases steeply towards lower energies with a small resonant maximum visible near 2.2 eV. Above 3 eV the TCS is dominated by second pronounced enhancement with the maximum (45×10^{-20} m^2) peaked near 9.5 eV. The experimental TCS findings are—at intermediate energies—satisfactorily reproduced with our total cross section estimation based on calculations of integral elastic (in independent atom approximation) and ionization (binary-encounter-Bethe approach) cross sections. The TCS measured for SO$_2$ClF is also compared with experimental TCSs for molecules containing sulfur as a central atom and it is found that some features observed for SO$_2$ClF are shared by others of the compared molecules.

1. Introduction

Investigations into how molecular structure is reflected in the magnitude and energy dependence of cross sections have been carried out since the beginning of systematic studies of electron scattering (e.g. Brüche (1927)). Finding such correlations would allow us to first, estimate values of quantities describing scattering for targets which are difficult to measure and/or calculate, and second, provide some insight into the role of target properties in the scattering process. In the course of our systematic study on the electron–molecule scattering we have found that some structural similarities of target molecules manifest in the similar TCS behaviour. For example, TCSs for molecules with the same central atom or the same

peripheral atoms show similar features (Szmytkowski *et al* 1998). That is especially evident for perfluorides—their TCSs demonstrate specific, very broad enhancement spanned between 20 and 100 eV—(e.g. Szmytkowski and Ptasińska-Denga (2001), Nishimura *et al* (2003)). On the other hand, the alteration to atoms arrangement in the molecule modifies essentially the character of TCS energy function at low energies (Szmytkowski and Kwitnewski 2002, 2003). To further understand how the presence and positioning of various atoms in the target molecule influence the electron scattering, we have extended our TCS measurements towards molecules containing a sulfur atom. Examination of electron impact data available for sulfurides, especially those with a sulfur atom placed in the centre of molecule, reveals that the energy location of features visible in their TCS curves is similar. One may presume, therefore, that such a similarity is related to the presence of sulfur, a common atom, in these molecules.

The main goal of the present study is to obtain absolute total electron-scattering cross section for sulfuryl chloride fluoride (SO_2ClF) molecule over a wide energy range. In addition, we want to check if the TCS features for SO_2ClF are shared by other sulfur containing molecules; the SO_2ClF molecule has sulfur as a central atom but differs in the external atoms and their settings from sulfurides studied so far. Finally, we applied simple theoretical formalisms to compute, first, intermediate-energy cross sections for elastic and ionization channels which, at these energies, contribute mostly to the scattering, and then, to obtain approximated total cross section values as a sum of the elastic and ionization constituents. Such data may be useful for modelling the gas phase reactions in plasma mixtures composed of sulfurides (Christophorou and Olthoff 2004).

Previous e^-–SO_2ClF investigations, available in the literature, are exceptionally scarce. Sullivan and Beauchamp (1978) have studied positive and negative fragment ions formation employing an ion cyclotron resonance technique. Fragment negative ions formed via dissociative attachment of slow electrons have been observed by Robbiani and Franklin (1979) and by Wang and Franklin (1980).

2. Experimental details

The experiment has been performed with the electrostatic electron spectrometer working in a linear transmission mode. The electron beam is formed and energy selected by a $127°$ cylindrical electrostatic monochromator in line with a system of electron lenses. The electrons of desired energy E ($\Delta E \sim 0.1$ eV, fwhm) are then directed into the reaction cell filled with the target molecules under study. The density of the target vapour held in the cell (40–100 mPa) is sufficiently low to assure single electron–molecule collision conditions. The electrons which cross over the reaction volume and emerge from the cell through the exit orifice are energy discriminated with the retarding field element which prevents inelastically scattered electrons being collected with a Faraday cup.

The total cross section, $Q(E)$, at each electron impact energy is derived by measuring an attenuation of the transmitted electron current in the reaction cell, and applying the Bouguer–de Beer–Lambert formula

$$Q(E) = \frac{k\sqrt{T_m T_c}}{pL} \ln \frac{I(E, 0)}{I(E, p)},$$

where $I(E, p)$ and $I(E, 0)$ are electron-beam intensities in the presence of target gas of the pressure p in the scattering cell or its absence ($p = 0$), respectively; L stands for the length of the electron trajectory in the cell, k is the Boltzmann constant. The temperature T_m of the mks capacitance manometer head is stabilized at 322 K, while the temperature of the scattering cell $T_c \leqslant T_m$ and slightly varies in the course of experiment; a pressure correction due to

the thermal transpiration effect (Knudsen 1910) is accounted for. The electron energy scale is established with reference to the resonant structure visible at around 2.3 eV when N$_2$ is admixtured. The uncertainty of the energy scale is estimated to be about 0.1 eV; nearly half of that value results from the influence of the SO$_2$ClF compound on the surface of electron optics elements.

In order to determine the energy dependence of TCS we took several series of measurements between 0.6 and 370 eV electron impact energy. The resulting TCS value at each energy is a weighted mean of results from series (4–13) of individual runs (typically 10 in series). The averages from 100 single readings of electron current intensities and the target pressure, respectively, are used for TCS evaluation in every single run. The overall statistical uncertainty of the final TCS is 1–1.5% below 2 eV and less than 1% over the remaining energy range investigated.

Preliminary runs showed annoying instability of the electron current when the target was supplied into the scattering cell. After few-day passivation of the electron optics and the sample inlet system with the target vapours, the current became sufficiently stable ($\Delta I / I \leqslant 0.005$) to carry out measurements and the TCS values obtained at the same energy appeared, within the random experimental uncertainties, independent of both the incident electron beam intensity (0.1–100 pA) and the applied target pressure. Other details of the setup and procedure employed in the present experiment can be found elsewhere (e.g. Szmytkowski *et al* (1998), Szmytkowski and Możejko (2001)).

The obtained TCS is also affected by systematic uncertainty. The main reasons of potential systematic deviation of the measured TCSs from the *true* TCS values are, in our transmission experiment, related to (i) the detection (as unscattered) of the electrons which are scattered elastically into the small-angle forward direction—this effect systematically lowers the obtained TCS; (ii) the effusion of target particles through the scattering orifices that causes an elongation of the path over which the scattering events take place, at that time the distribution of target density in the vicinity of orifices becomes highly inhomogeneous; (iii) the shift in the energy scale in the course of experiment due to reactivity of target particles with the surface of the electron optics elements that leads to broadening and flattening of sharp features in the TCS energy dependence and (iv) the presence of impurities in the scattering volume—commercial sample of SO$_2$ClF was used as received from supplier (Aldrich, at least 94% purity) aside from several freeze-pump-thaw degassing cycles. To find the impurities which can bias the measured TCS value, the mass spectrometry analysis of the degassed SO$_2$ClF sample in the target driving system has been carried out. The mass spectra revealed only the positive parent ions as well as those which may originate from the parent molecule decomposition; relative abundances of ions were in good agreement with those obtained by Sullivan and Beauchamp (1978). The final TCS results are not corrected with regards to aforementioned effects. The estimated overall systematic uncertainty in our measured absolute cross sections amounts up to 7–9% below 2 eV, is 4–5% in the vicinity of the main TCS maximum and 5–7% above 100 eV.

3. Calculations

The theoretical methods and computational issues employed in the present calculations have been described in detail in our previous works (e.g. Możejko *et al* (2002), Możejko and Sanche (2005), Szmytkowski *et al* (2005)), hence only a brief description of applied procedures is given here.

Cross sections for elastic scattering of 40–4000 eV electrons from SO$_2$ClF molecules have been obtained applying the independent atom method (IAM) (Mott and Massey 1965)

with a static and polarization model potential. In the IAM approach the integral cross section for elastic scattering of electrons, at impact energy E, is given by

$$\sigma(E) = \frac{4\pi}{k} \sum_{i=1}^{N} \mathrm{Im}\, f_i(\theta = 0, k) = \sum_{i}^{N} \sigma_i(E), \tag{1}$$

where $f_i(\theta, k)$ is the complex scattering amplitude due to the ith atom of the molecule, θ is the scattering angle, $k = \sqrt{2E}$ is the wave number of the incident electron and N is the number of atoms within the molecule; $\sigma_i(E)$ is the integral elastic cross section of the ith atom of the target molecule. For the convenience, in all equations regarding elastic scattering, we adopted atomic units in which $e = m = \hbar = 1$, although all presented and discussed results of our computations are given in the SI units.

The elastic electron–atom cross sections have been derived making partial wave analysis and solving numerically the radial Schrödinger equation

$$\left(\frac{\mathrm{d}^2}{\mathrm{d}r^2} - \frac{l(l+1)}{r^2} - 2(V_{\mathrm{stat}}(r) + V_{\mathrm{polar}}(r)) + k^2 \right) u_l(r) = 0 \tag{2}$$

under the boundary conditions

$$u_l(0) = 0, \qquad u_l(r) \xrightarrow{r \to \infty} A_l \hat{J}_l(kr) - B_l \hat{n}_l(kr), \tag{3}$$

where $\hat{j}_l(kr)$ and $\hat{n}_l(kr)$ are the spherical Bessel–Riccati and Neumann–Riccati functions, respectively. $V_{\mathrm{stat}}(r)$ is the static potential of the atom determined following the procedure of Salvat *et al* (1987):

$$V_{\mathrm{stat}}(r) = -\frac{Z}{r} \sum_{i=1}^{3} a_i \exp(-\beta_i r), \tag{4}$$

where Z is the nuclear charge and β_i and a_i are the parameters, determined by an analytical fitting procedure to Dirac–Hartree–Fock–Slater self-consistent data (Salvat *et al* 1987). The polarization potential $V_{\mathrm{polar}}(r)$ is expressed in the form proposed by Padial and Norcross (1984):

$$V_{\mathrm{polar}}(r) = \begin{cases} v(r) & r \leqslant r_c \\ -\alpha/2r^4 & r > r_c, \end{cases} \tag{5}$$

where $v(r)$ is the free-electron-gas correlation energy (Pedrew and Zunger 1981) and α is the static electric dipole polarizability of atom; the r_c is the first crossing point of the $v(r)$ and $-\alpha/2r^4$ curves (Zhang *et al* 1992).

Electron-impact ionization cross sections for electron energies ranging from threshold up to 4000 eV have been obtained using the binary-encounter-Bethe (BEB) formalism (Hwang *et al* 1996). According to BEB approach the electron-impact ionization cross section per molecular orbital is given by

$$\sigma^{\mathrm{BEB}} = \frac{S}{t + u + 1} \left[\frac{\ln t}{2} \left(1 - \frac{1}{t^2} \right) + 1 - \frac{1}{t} - \frac{\ln t}{t + 1} \right], \tag{6}$$

where $S = 4\pi a_0^2 N R^2 / B^2$, $u = U/B$, $t = T/B$ and T is the energy of the impinging electron ($a_0 = 0.5292$ Å, $R = 13.61$ eV). All molecular parameters and properties necessary for cross section calculations, like optimized molecular geometry, the electron binding energy, B, the kinetic energy of the orbital, U, and orbital occupation number, N, were obtained for the ground state of the molecule with the Hartree–Fock method using the GAMESS code (Schmidt *et al* 1993), and Gaussian 6-311G basis set. Moreover, for further analysis of the experimental TCS data, lowest unoccupied molecular orbital (LUMO) energies and electric dipole moment
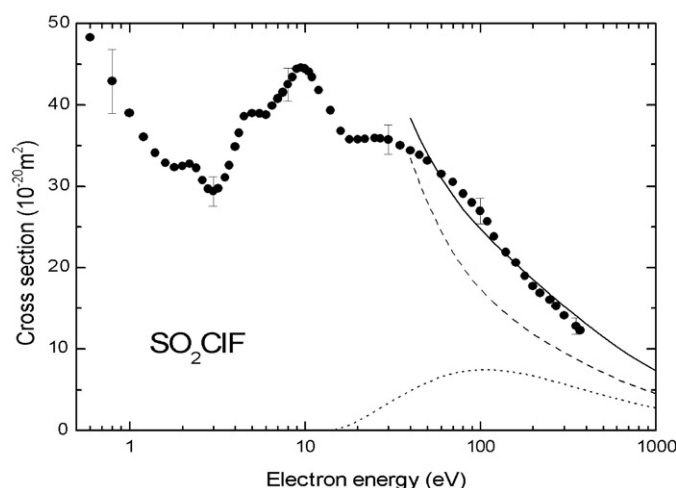
Figure 1. Energy dependence of cross sections for electron–SO$_2$ClF scattering (present results): experimental TCS (●), error bars represent overall (statistical + systematic) experimental uncertainties; ——, calculated TCS (elastic + ionization). Calculated partial cross sections: - - - -, integral elastic (ECS); ······, ionization (ICS).

of the molecule studied have been calculated with the same method. To fix the threshold behaviour of calculated ionization cross section at the experimental value, the first ionization potential (12.6 eV) taken from the measurements of Mines *et al* (1972) was inserted in the calculations, instead that obtained theoretically (14.09 eV). Finally, the total cross section for electron-impact ionization, σ_{ion}, was obtained as the sum of σ^{BEB} for all occupied molecular orbitals.

4. Results and discussion

Figure 1 shows the absolute electron–SO$_2$ClF scattering *grand* TCS we have obtained in this work at energies ranging from 0.6 to 370 eV using the electron-transmission method. In the same figure, the intermediate-energy theoretical *total* cross section which is a sum of our calculated integral elastic (ECS) and ionization (ICS) cross sections is also displayed for comparison. Table 1 presents the numerical e$^-$–SO$_2$ClF experimental TCS values while the computed ECS and ICS values are listed in table 2.

Most noticeable characteristic of the obtained TCS energy dependence is a variety of more or less marked features in its low-energy part, while the intermediate-energy tail (beyond 30 eV) of the TCS energy function declines smoothly as the energy increases. The interpretation of low-energy TCS variability is possible only in part as more detailed experimental studies and theoretical investigations of e$^-$–SO$_2$ClF scattering in this energy range are missing. Therefore, to better elucidate the observed features we refer to some similarities visible both in TCSs for SO$_2$ClF molecule and for other molecular targets with the central sulfur atom. To illustrate these similarities, in figure 2 we have gathered the TCS results for selected sulfur-containing molecules (majority of presented data have been taken in our laboratory) while in table 3 the energy location of the most prominent TCS low-energy features in such compounds is specificated. The intermediate-energy experimental TCS for SO$_2$ClF appeared to be quite satisfactorily interpreted through the contribution of elastic and ionization components only.

Table 1. Experimental absolute total cross section (TCS) for electron scattering from sulfuryl chloride fluoride (SO_2ClF) molecules (in units of 10^{-20} m^2).

Energy (eV)	TCS	Energy (eV)	TCS	Energy (eV)	TCS	Energy (eV)	TCS
0.6	48.3	4.0	34.9	12	41.8	90	28.0
0.8	42.9	4.2	36.6	14	39.4	100	27.0
1.0	39.0	4.5	38.6	16	36.8	110	25.7
1.2	36.1	5.0	39.0	18	35.8	120	23.8
1.4	34.1	5.5	39.0	20	35.8	140	21.9
1.6	32.9	6.0	38.8	22	35.9	160	20.6
1.8	32.4	6.5	39.9	25	36.0	180	19.0
2.0	32.5	7.0	40.8	27	35.9	200	17.7
2.2	32.8	7.5	41.6	30	35.8	220	16.9
2.4	32.4	8.0	42.5	35	35.1	250	16.0
2.6	30.8	8.5	43.4	40	34.4	270	15.3
2.8	29.7	9.0	44.4	45	33.9	300	14.1
3.0	29.4	9.5	44.6	50	33.2	350	12.8
3.2	29.8	10.0	44.4	60	31.5	370	12.3
3.5	31.1	10.5	44.1	70	30.5		
3.7	32.6	11.0	43.4	80	29.1		

Table 2. Ionization (ICS) and integral elastic (ECS) cross sections calculated for electron impact on SO_2ClF molecule (in units of 10^{-20} m^2).

Energy (eV)	ICS	Energy (eV)	ICS	ECS	Energy (eV)	ICS	ECS
12.6	0.00	40	4.91	33.5	250	6.18	10.5
13.0	0.0186	45	5.47	30.5	300	5.72	9.54
14.0	0.0678	50	5.92	28.1	350	5.32	8.75
15.0	0.122	60	6.57	24.4	400	4.96	8.10
16.0	0.277	70	6.97	21.9	450	4.65	7.56
17.0	0.483	80	7.22	20.0	500	4.38	7.09
18.0	0.690	90	7.36	18.5	600	3.92	6.34
19.0	0.913	100	7.42	17.4	700	3.55	5.75
20.0	1.15	110	7.43	16.4	800	3.25	5.27
22.5	1.75	120	7.40	15.7	900	3.00	4.87
25.0	2.35	140	7.28	14.4	1000	2.78	4.54
27.5	2.89	160	7.10	13.4	2000	1.66	2.81
30.0	3.39	180	6.90	12.6	3000	1.20	2.19
35.0	4.23	200	6.69	11.9	4000	0.949	2.00

As seen in figure 1, at the lowest energies used the measured e^-–SO_2ClF TCS rapidly decreases from about 48×10^{-20} m^2 at 0.6 eV down to slightly below 30×10^{-20} m^2 near 3 eV, where the TCS curve reaches its deep minimum. It is well known that such behaviour of the low-energy TCS curve may be explained, at least in part, in terms of direct scattering of electrons from target possessing the permanent electric dipole moment—slower electron spends more time in a long-distant field of polar molecule what manifests in the increase of the low-energy cross section. The SO_2ClF molecule, due to its structural asymmetry (see figure 3), is polar in the ground state. Its electric dipole moment calculated in the present work is relatively high and amounts about 1.9 D. This value reasonably agrees with the rough
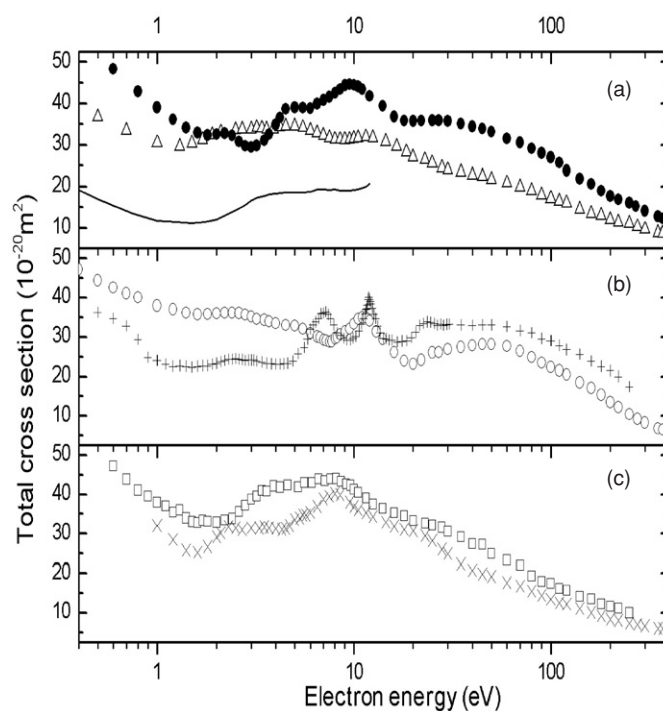
Figure 2. Comparison of experimental electron-scattering TCSs for some sulfur-containing molecules: (a) SO$_2$ClF (•, present); SO$_2$ (△, Szmytkowski *et al* (2003)); SO$_2$F$_2$ (——, Wan *et al* (1993)); (b) SF$_4$ (○, Szmytkowski *et al* (2005)); SF$_6$ (+, Kasperski *et al* (1997)); (c) H$_2$S (×, Szmytkowski and Maciąg (1986), Szmytkowski *et al* (2003)); CH$_3$SH (□, Szmytkowski *et al* (1995)).
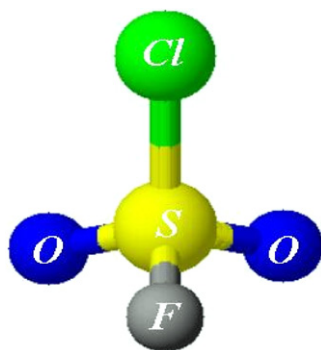

Figure 3. Schematic diagram of the SO$_2$ClF molecular geometry.

estimation (1.5 D) deduced from data available for other molecules containing Cl and/or F atoms (Lide 2004–2005); from comparison it results that the dipole moment for molecules with single Cl and F atoms lies in between the moments for their counterparts with two Cl atoms and those with two F atoms. Figure 2 shows that similar TCS increase towards zero energy is visible for other polar sulfur-containing molecules, although—what is worth noting—the same behaviour demonstrates also TCS for nonpolar SF$_6$ molecule.

Table 3. Location of the features discernible in TCS energy dependences (see figure 2) for some sulfur-containing molecules.

Molecule		(eV)		
SO_2ClF	2.2	4–5	9.5	25
SO_2	3.4	5–6	12	25
SO_2F_2		4–6		
SF_4	2.3	4–5	11	25
SF_6	2.5	7.2	12	23
SH_2	2.3	4–5	9	23
$SHCH_3$	2.8	4–5	8	23

On the low-energy TCS slope, near 2.2 eV, some small but quite distinct peak is superimposed. There are some indications that this feature may be attributed to the indirect e^-–SO_2ClF scattering—occurring via transient negative-ion state formation when the projectile electron is temporarily trapped by target molecule into normally vacant orbital. Direct evidence for resonant origin of the 2.2 eV peak comes from the observation of fragment negative ions (F^-, Cl^-, SO_2F^- and ClF^-) around 2.5–2.6 eV (Wang and Franklin 1980). Further, our calculations show that the lowest unoccupied molecular orbital of SO_2ClF, to which the approaching electron could be attached, is located just at 2 eV. Indirect argument on the resonant character of the 2.2 eV peak follows from the inspection of electron-scattering data for targets with the central sulfur atom. TCSs for sulfur-containing molecules also show some weak features located between 2 and 3.5 eV (cf figure 2 and table 3). The experiments carried out in vibrational (e.g. Rohr (1978), Andrić *et al* (1983), Cho *et al* (2000); for more references see Karwasz *et al* (2001)) and/or dissociative attachment channels (e.g. Kraus (1961), Wan *et al* (1993)) revealed that the 2–3 eV TCS structures for SO_2, H_2S and SF_6 are resonant in origin. The presence of resonances in that energy regime has been also confirmed in theoretical calculations of Jain and Thompson (1983) and Gianturco (1991) for H_2S, by Andrić *et al* (1983) for SO_2 and by Dehmer *et al* (1978) for SF_6.

In the range of 3–4.5 eV the TCS for SO_2ClF sharply increases and shows a distinct shoulder located between 4 and 6 eV. Calculations demonstrate the presence of vacant orbitals of the SO_2ClF molecule in this energy regime to which impinging electron can be attached. Some features centred near 5 eV are also visible in TCS for other sulfurides: as a weak hump in TCS for SO_2, and as a shoulder for SO_2F_2, SF_4, CH_4S and H_2S molecules. Again, comparison with experimental and theoretical results on electron-scattering from sulfur-containing targets: SO_2 (Kraus 1961, Wan *et al* 1993, Gianturco *et al* 1997), SO_2F_2 (Wan *et al* 1993), H_2S (Kraus 1961, Gianturco 1991) and SF_6 (Lehmann 1970) may suggest the contribution of resonant effects in this energy range also for SO_2ClF molecule.

Beyond 6 eV the TCS increases again and at 9.5 eV it reaches its maximum value of nearly 45×10^{-20} m^2. The enhancement around 9.5 eV is most likely related to the substantial increase of the yield of the elastic scattering in this energy range, mainly in the direct scattering channel, although, some contribution of resonant effects cannot be excluded. From 10 to 20 eV the TCS decreases and at 25 eV it has a small hump, similar to that visible in the TCS curves for SF_4, SF_6 and H_2S molecules. Calculations of Dehmer *et al* (1978) and Gianturco *et al* (1995) point out that for SF_6 molecule the 25 eV feature is mainly atomic in character and is associated with the central sulfur atom. One might believe, therefore, that the origin of that structure in the SO_2ClF curve is the same.

Above 25 eV the TCS becomes the descending function of energy, which may be described with the regression formula $Q \sim E^{-a}$, where $a \simeq 0.5$. Such an energy dependence means that the TCS is just proportional to the time needed for the projectile to pass the distance equal

to the size of target molecule. Between 60 and 120 eV some weak buldge in the TCS curve extends, related to rapidly increasing role of the ionization. At the highest energy employed in our experiment, at 370 eV, the TCS falls down to about 12×10^{-20} m^2; as computations show, nearly 40% of this value is related to ionization.

Figure 1 clearly demonstrates that for energies above 50 eV the measured TCS is reasonably reproduced with the sum of calculated integral elastic (in independent atom approximation) and ionization cross sections (binary-encounter-Bethe approach)—differences do not exceed 10% over whole 50–370 eV energy range. Such an agreement indicates that the approximations used in the present work are suitable for rough estimation of partial and total electron-scattering cross sections at intermediate energies. Between 60 and 120 eV the experiment is slightly higher than computations while above 180 eV that relation reverses. Below 50 eV the disagreement between experiment and computations rapidly increases. At such low energies the wavelength of the incident electron becomes comparable with separation between constituents of target molecule and the assumptions of the independent atom approximation are not valid any longer.

5. Conclusion

We have measured the absolute total cross section for electron scattering by SO$_2$ClF molecules using a linear transmission method, over the energy range 0.6–370 eV. In the low-energy part of the TCS numerous resonant-like features are discernible. The most pronounced TCS features are two enhancements separated with a deep minimum located at 3 eV. The TCS increase below 3 eV, related to direct scattering, is superimposed with a weak resonant peak near 2.2 eV. The broad enhancement peaked around 9.5 eV has additive features on its both sides: a shoulder between 4 and 6 eV, and a small hump near 25 eV. These features are located in energy ranges where some resonant structures in TCSs for other sulfur-containing molecules have already been observed. Our calculated total cross section (elastic + ionization) reproduces quite satisfactorily the experimental intermediate-energy TCS data. Some similarities between electron-impact TCS for SO$_2$ClF and the data for other sulfurides are also pointed out and discussed; they suggest a significant role of the central atom—sulfur—in the electron scattering from these compounds. For more convincing explanation of the low-energy features in the TCS for SO$_2$ClF molecule, further experimental and theoretical investigations are necessary.

Acknowledgments

References

Andrić L, Čadež I, Hall R I and Zubek M 1983 *J. Phys. B: At. Mol. Phys.* **16** 1837–51
Brüche E 1927 *Ann. Phys., Lpz.* **83** 1065–128
Cho H, Gulley R J, Trantham K W, Uhlmann L J, Dedman C J and Buckman S J 2000 *J. Phys. B: At. Mol. Opt. Phys.* **33** 3531–44
Christophorou L G and Olthoff J K 2004 *Fundamental Electron Interactions with Plasma Processing Gases* (New York: Kluwer/Plenum)
Dehmer J L, Siegel J and Dill D 1978 *J. Chem. Phys.* **69** 5205–6
Gianturco F A 1991 *J. Phys. B: At. Mol. Opt. Phys.* **24** 4627–48
Gianturco F A, Lucchese R R and Sanna N 1995 *J. Chem. Phys.* **102** 5743–50
Gianturco F A, Paioletti P and Sanna N 1997 *J. Phys. B: At. Mol. Opt. Phys.* **30** 4535–57

Hwang W, Kim Y K and Rudd M E 1996 *J. Chem. Phys.* **104** 2956–66
Jain A and Thompson D G 1983 *J. Phys. B: At. Mol. Phys.* **17** 443–60
Karwasz G P, Brusa R S and Zecca A 2001 *Riv. Nuovo Cimento* **24** 1–118
Kasperski G, Możejko P and Szmytkowski Cz 1997 *Z. Phys.* D **42** 187–91
Knudsen M 1910 *Ann. Phys., Lpz.* **31** 205–29
Kraus K 1961 *Z. Naturf.* A **16** 1378–85
Lehmann B 1970 *Z. Naturf.* A **25** 1755–7
Lide D R (ed) 2004–2005 *CRC Handbook of Chemistry and Physics* 85th edn (Boca Raton, FL: CRC Press)
Mines G W, Thomas R K and Thompson H 1972 *Proc. R. Soc.* A **329** 275–82
Mott N F and Massey H S W 1965 *The Theory of Atomic Collisions* (Oxford: Oxford University Press)
Możejko P and Sanche L 2005 *Radiat. Phys. Chem.* **73** 77–84
Możejko P, Żywicka-Możejko B and Szmytkowski Cz 2002 *Nucl. Instrum. Methods Phys. Res.* B **196** 245–52
Nishimura H, Nishimura F, Nakamura Y and Okuda K 2003 *J. Phys. Soc. Japan* **72** 1080–6
Padial N T and Norcross D W 1984 *Phys. Rev.* A **29** 1742–8
Pedrew J P and Zunger A 1981 *Phys. Rev.* B **23** 5048–79
Robbiani R and Franklin J L 1979 *J. Am. Chem. Soc.* **101** 3709–15
Rohr K 1978 *J. Phys. B: At. Mol. Phys.* **11** 4109–17
Salvat F, Martinez J D, Mayol R and Parellada J 1987 *Phys. Rev.* A **36** 467–74
Schmidt M W *et al* 1993 *J. Comput. Chem.* **14** 1347–63
Sullivan S A and Beauchamp J L 1978 *Int. J. Mass Spectrom. Ion Phys.* **28** 69–80
Szmytkowski Cz, Domaracka A, Możejko P, Ptasińska-Denga E and Kwitnewski S 2005 *J. Phys. B: At. Mol. Opt. Phys.* **38** 745–55
Szmytkowski Cz, Kasperski G and Możejko P 1995 *J. Phys. B: At. Mol. Opt. Phys.* **28** L629–32
Szmytkowski Cz and Kwitnewski S 2002 *J. Phys. B: At. Mol. Opt. Phys.* **35** 3781–90
Szmytkowski Cz and Kwitnewski S 2003 *J. Phys. B: At. Mol. Opt. Phys.* **36** 4865–73
Szmytkowski Cz and Maciąg K 1986 *Chem. Phys. Lett.* **124** 463–6
Szmytkowski Cz and Możejko P 2001 *Vacuum* **63** 549–54
Szmytkowski Cz, Możejko P and Kasperski G 1998 *J. Phys. B: At. Mol. Opt. Phys.* **31** 3917–28
Szmytkowski Cz, Możejko P and Krzysztofowicz A 2003 *Rad. Phys. Chem.* **68** 307–11
Szmytkowski Cz and Ptasińska-Denga 2001 *Vacuum* **63** 545–48
Wan H-X, Moore J H, Olthoff J K and van Brunt R J 1993 *Plasma Chem. Plasma Process* **13** 1–16
Wang J-S and Franklin J L 1980 *Int. J. Mass Spectrom. Ion Phys.* **36** 233–47
Zhang X, Sun J and Liu Y 1992 *J. Phys. B: At. Mol. Opt. Phys.* **25** 1893–7